

OPEN

Transplantation of Human-induced Pluripotent Stem Cell-derived Cardiomyocytes Is Superior to Somatic Stem Cell Therapy for Restoring Cardiac Function and Oxygen Consumption in a Porcine Model of Myocardial Infarction

Masaru Ishida, MD,¹ Shigeru Miyagawa, MD, PhD,¹ Atsuhiko Saito, PhD,² Satsuki Fukushima, MD, PhD,¹ Akima Harada,¹ Emiko Ito, PhD,¹ Fumiya Ohashi,¹ Tadashi Watabe, MD, PhD,³ Jun Hatazawa, MD, PhD,³ Katsuhisa Matsuura, MD, PhD,⁴ and Yoshiki Sawa, MD, PhD¹

Background. Somatic stem cell (SC) therapy can improve cardiac performance following ischemic injury. In this study, we investigated whether induced pluripotent SC-derived cardiomyocytes (iPS-CMs) are more effective than somatic SCs, such as skeletal myoblasts (SM) and mesenchymal (M)SCs, in promoting functional recovery upon transplantation in a porcine model of myocardial infarction. **Methods.** Myocardial injury was induced by ameroid ring placement in immunosuppressed female mini pigs; after 1 month, epicardial cell transplantation was performed with iPS-CMs (n = 7), SMs (n = 7), and MSCs (n = 7). Control pigs underwent sham operation (n = 8). **Results.** Cell therapy improved functional recovery 2 months after myocardial infarction, as evidenced by increased ejection fraction (iPS-CM, +7.3% ± 2.2% and SM, +5.8% ± 5.4% vs control, -4.4% ± 3.8%; *P* < 0.05). The analysis of regional contractile function in the infarcted zone revealed an increase in transverse peak strain (iPS-CM, +4.6% ± 2.2% vs control, -3.8% ± 4.7%; *P* < 0.05). The C-11 acetate kinetic analysis by positron emission tomography showed that the work-metabolic cardiac energy efficacy increased by the transplantation of iPS-CMs, but was reduced by the other cell types. This was accompanied by decreased myocardial wall stress in the infarcted zone (iPS-CM, -27.6 ± 32.3 Pa and SM, -12.8 ± 27 Pa vs control, +40.5 ± 33.9 Pa; *P* < 0.05). **Conclusions.** The iPS-CM is superior to other somatic cell sources in terms of improving regional contractile function and cardiac bioenergetic efficiency, suggesting greater clinical benefits in severely damaged myocardium.

(*Transplantation* 2019;103: 291–298)

The heart was formerly considered as a terminally differentiated organ lacking regenerative capacity. The discovery of endogenous cardiac progenitor cells and reports

of low turnover of existing cardiomyocytes (CMs) have altered this view.¹ However, the adult heart tissue cannot replace myocytes that are lost after injury as tissue

Received 4 October 2017. Revision received 30 June 2018.

Accepted 4 July 2018.

¹ Division of Surgery, Department of Cardiovascular Surgery, Faculty of Medicine, Osaka University Graduate School of Medicine, Osaka, Japan.

² Medical Center for Translational Research, Osaka University Hospital, Osaka, Japan.

³ Department of Nuclear Medicine and Tracer Kinetics, Osaka University Graduate School of Medicine, Osaka, Japan.

⁴ Institute of Advanced Biomedical Engineering and Science, Tokyo Women's Medical University, Shinjuku, Tokyo, Japan.

This study was supported by the Research Center Network for Regenerative Medicine from the Japan Agency for Medical Research and Development (AMED).

K.M. is an inventor of bioreactor systems. The authors declare no conflicts of interest.

M.I. performed all the experiments, analyzed all the data, wrote the article, and prepared the figures. S.M. helped to set up all the experiments and contributed to data analysis. A.S. and S.F. contributed to the experimental design. A.H., E.I., and

F.O. provided advice for cell culture and histopathological experiments. T.W. and J.H. contributed to the analysis of cardiac oxygen consumption in experimental animals by positron emission tomography scanning. K.M. supplied induced pluripotent stem cell-derived cardiomyocytes. Y.S. is the corresponding author and helped the first author design the technical aspects of the experiments.

Correspondence: Yoshiki Sawa, Division of Surgery, Department of Cardiovascular Surgery, Faculty of Medicine, Osaka University Graduate School of Medicine, 2-2 Yamadaoka, Suita, Osaka 565-0871, Japan. (sawa-p@surg1.med.osaka-u.ac.jp).

Supplemental digital content (SDC) is available for this article. Direct URL citations appear in the printed text, and links to the digital files are provided in the HTML text of this article on the journal's Web site (www.transplantjournal.com).

Copyright © 2018 The Author(s). Published by Wolters Kluwer Health, Inc. This is an open-access article distributed under the terms of the Creative Commons Attribution-Non Commercial-No Derivatives License 4.0 (CCBY-NC-ND), where it is permissible to download and share the work provided it is properly cited. The work cannot be changed in any way or used commercially without permission from the journal.

ISSN: 0041-1337/19/10302-0291

DOI: 10.1097/TP.0000000000002384

regeneration occurs very slowly. Accordingly, a significant loss of myocardium due to ischemic injury or disease can lead to progressive heart failure.² Despite pharmacological advances, including the development of beta blockers and renin angiotensin system inhibitors, the treatment for refractory heart failure remains a challenge.

Cell-based therapy using adult stem cells (SCs) offers the possibility to restore cardiac function.³⁻⁵ However, there is an ongoing debate regarding the optimal cell source for cardiac repair. Embryonic SC-derived CMs may be suitable in small animal models.^{6,7} However, to the best of our knowledge, no study has compared the CMs and other types of somatic SC in terms of their effectiveness for cell-based therapy. Induced pluripotent SCs (iPS) with the ability to differentiate into CMs have recently been developed.^{8,9} They provide an unlimited cell source to repair damaged cardiac tissue without ethical concerns.^{10,11}

In this study, we investigated whether iPS cell-derived CMs (iPS-CMs) are superior to other types of somatic cells, such as skeletal myoblasts (SMs) and bone marrow-derived mesenchymal (M)SCs, in terms of promoting functional recovery and cardiac bioenergetics in a porcine model of myocardial infarction (MI).

MATERIALS AND METHODS

Generation of Cell Sheets

The iPS-CMs used in this study were previously developed.¹² The human MSCs (Lonza Japan, Tokyo, Japan) and human SMs (Lonza Japan) were cultured according to the instruction of the manufacturer. The cells were cultured at 1×10^7 /dish in a 100-mm culture dish (UpCell; CellSeed, Tokyo, Japan) whose surface was coated with a temperature-responsive polymer (poly-N-isopropylacrylamide). After 1 week, the dishes were transferred to a 20°C incubator, which caused the cells to spontaneously detach as a scaffold-free cell sheet. Ten cell sheets each containing 1×10^8 cells were prepared from each animal.

Porcine Model of Ischemic Injury and Cell Transplantation

The Animal Care Committee of the Osaka University Graduate School of Medicine approved the experimental protocol (Figure S1, SDC, <http://links.lww.com/TP/B613>). All procedures involving animals were performed according to the animal use guidelines of the University of Osaka and were consistent with the National Institute of Health's Guide of the Care and Use of Laboratory Animals (National Institutes of Health publication no. 85-23, revised 1985). Myocardial infarction was induced in adult female CLAWN miniature porcine (weighing 18-25 kg; Kagoshima Miniature Swine Research Swine Center, Kagoshima, Japan) by fitting an ameroid constrictor to the proximal left descending coronary artery; the detailed procedure can be found in SDC, Materials and Methods, <http://links.lww.com/TP/B613>. One month after MI, the animals were randomly assigned to 1 of the 3 cell therapy groups—iPS-CM (MI with 1×10^8 iPS-CMs; $n = 7$); SM (MI with 1×10^8 SMs; $n = 7$); and MSC (MI with 1×10^8 MSCs; $n = 7$)—or a control group (MI with sham operation; $n = 8$). The cell sheets were placed to cover the infarcted and surrounding border areas. The animals in the control group underwent the same surgical procedure, except for cell sheet placement. As

transplanted cells were derived from human tissue, the animals were injected with the following immunosuppressants: tacrolimus (5 mg during the operation), followed by a triple-drug regimen of tacrolimus (1 mg/kg per day), mycophenolate mofetil (500 mg/d), and corticosteroids (20 mg/day as a food supplement).

Cardiac Contractility, Left Ventricle Hemodynamics, and Histological Assessment

The cardiac function was evaluated by magnetic resonance imaging (MRI) and echocardiography as summarized in SDC, Materials and Methods, (<http://links.lww.com/TP/B613>). The MRI was performed with a 1.5-T clinical scanner (Signa EXCITE XI TwinSpeed 1.5 T v.11.1; GE Healthcare, Milwaukee, WI). The infarcted area was visualized by delayed enhancement. An infarcted zone (IZ)/lateral border zone (BZ)/remote zone (RZ) segmentation scheme was used to analyze regional function, with IZ, BZ, and RZ defined in the delayed enhancement images (Figure S2, SDC, <http://links.lww.com/TP/B613>). Echocardiography was performed with a commercially available system (Aplio Artida; Toshiba Medical Systems, Tokyo, Japan). The left ventricle (LV) hemodynamics was monitored with a catheter inserted into the LV via the apical dimple. The histological assessment was carried out according to a standard protocol.

Cardiac Oxygen Consumption

In vivo measurement of myocardial oxygen consumption was performed using a positron emission tomography (PET) scanner (Headtome-V SET2400W; Shimadzu, Kyoto, Japan) after a bolus injection of 370 MBq ¹¹C acetate (Figure S3, SDC, <http://links.lww.com/TP/B613>). The animals were sedated by propofol infusion (5 mL/h) and with 1% isoflurane inhalation, and were positioned in a whole-body PET scanner at the PET Molecular Imaging Center of Osaka University Graduate School of Medicine. A 15-min transmission scan was performed to correct emission images for photon attenuation. Immediately after the transmission scan, 370 MBq of ¹¹C acetate was administered intravenously, and dynamic PET acquisition was initiated (15 min). The measurements were performed under both rest condition and in a high cardiac work state induced by catecholamine (dobutamine, 20 µg/kg per minute). The PET images were acquired in 30 frames (10 s × 6, 20 s × 6, 30 s × 12, and 60 s × 6) and reconstructed with the filtered back projection algorithm. The blood pressure and heart rate (HR) were monitored during the scan. To determine the global cardiac oxygen consumption, the acetate clearance rates (myocardial oxidative consumption [k_{mono}]) of all segments of each measurement were averaged. The cardiac efficiency (CE) was calculated using the concept of work metabolic index according to the formula $\text{CE} = \text{stroke volume (in mL)} \times \text{systolic blood pressure (in mm Hg)} \times \text{HR} / k_{\text{mono}}$.

Statistical Analyses

The data are reported as mean ± standard error of mean and were analyzed with the JMP Pro v.12.0 software (SAS Institute, Tokyo, Japan). Differences among the groups were evaluated by the one-way analysis of variance, and the experimental groups were compared at different time points by the 2-way repeated-measures analysis of variance. When a significant effect was detected, we performed Tukey-Kramer post hoc analysis to determine significance for specific

comparisons at each time point. The values for different experimental conditions within a group were compared to the baseline by paired *t* test. Comparisons between groups were performed by unpaired *t* test. Statistical significance was determined as $P < 0.05$.

RESULTS

Characteristics of Transplanted Cells and Cell Sheets

The purity of cardiomyocytes in the final iPS-CM culture was ~70%, as determined by the flow cytometric detection of cardiac troponin T (cTnT) (Figure 1A). Intercellular junctions and adhesive proteins were well preserved in the iPS-CM sheets. Fluorescence immunostaining revealed that the human iPS-CM expressed cTnT (Figure 1B) and alpha-sarcomeric actinin (Figure 1C). The purity of SMs was as high as 70% when evaluated via the flow cytometry analysis of the skeletal muscle SC marker cluster of differentiation (CD)56 (Figure 1E). Most of the SMs expressed fast-myosin heavy chain (Figure 1F) and desmin (Figure 1G), determined via fluorescence immunostaining. The MSCs displayed high expression of CD105 surface antigen (average 80%) when evaluated via the flow cytometry analysis (Figure 1I), and

expressed CD105 (Figure 1J) and CD90 (Figure 1K) when evaluated via fluorescence immunostaining.

iPS-CM Transplantation Improves Global and Regional Cardiac Functions After MI

Cardiac function was assessed by echocardiogram and the animals with impaired LV systolic function, ie, an LV ejection fraction (LVEF) $< 50\%$ 1 month after induction of MI, were assigned to 1 of the 4 experimental groups. Six animals with the LVEF $> 50\%$ were excluded. During ameroid ring placement, 11 pigs died of hemorrhage or ventricular fibrillation, and 3 died of cardiac arrhythmia in the first month after MI induction. The remaining 29 animals were randomly assigned to the iPS-CM ($n = 7$), SM ($n = 7$), MSC ($n = 7$), and sham (MI only, $n = 8$) groups. The impairment in systolic function prior to treatment was relatively uniform across the groups (Figure 2A). We successfully performed the treatments and there was no mortality due to the procedure or otherwise prior to the planned sacrifice.

Global Cardiac Function

To assess the global left ventricular function, we performed cardiac MRI and echocardiography (Figure 1 and Figure S4,

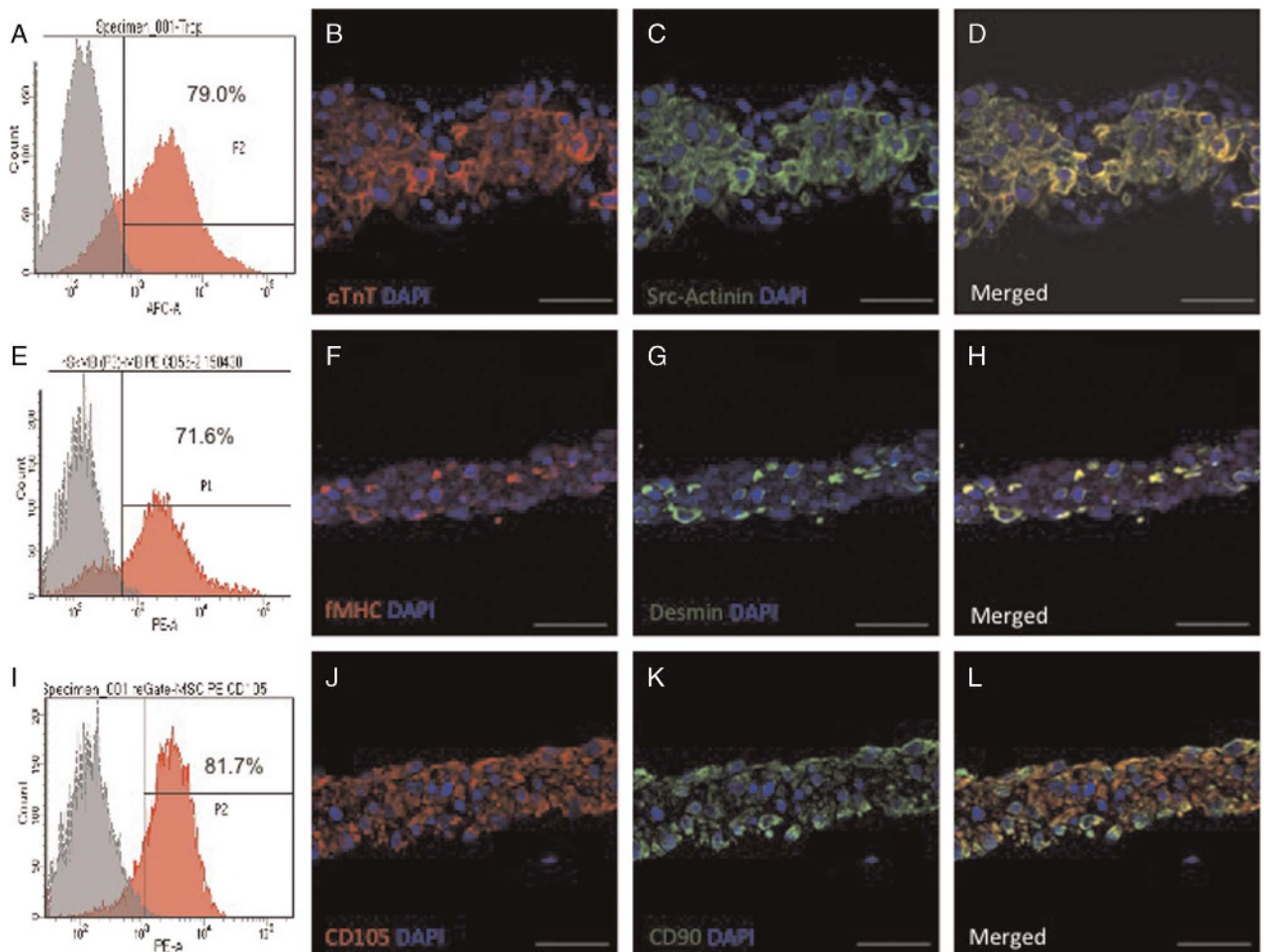


FIGURE 1. Characterization of the induced pluripotent SC-derived cardiomyocytes (iPS-CM), skeletal myoblast (SM), and mesenchymal stem cell sheets. A, Flow cytometry analysis of cardiac troponin T (cTnT) expression in the iPS-CMs. B–D, Representative image of cTnT, B, and alpha-sarcomeric actinin (C) in the iPS-CM sheets detected by fluorescence immunolabeling; nuclei were counterstained with 4',6-diamidino-2-phenylindole (DAPI). E, Flow cytometry analysis of CD56 expression in the SM cells. F–H, Representative images of the SM sheets expressing fast-myosin heavy chain (F) and desmin (G). I, Flow cytometry analysis of CD105 expression in the MSCs. (J–L) Representative image of MSC sheet expressing CD105 (J) and CD90 (K). D, H, L, Merged images are shown. Scale bar, 50 μm .

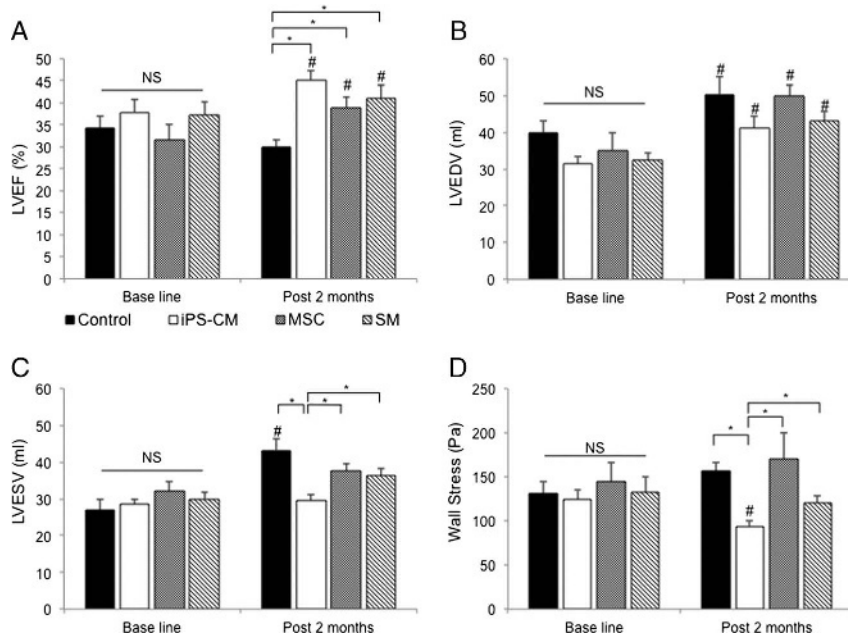


FIGURE 2. Effects of the transplanted induced pluripotent SC-derived cardiomyocytes (iPS-CM), skeletal myoblast (SM), and mesenchymal stem cell sheets on global cardiac function. A–D, Cardiac MRI results (infarcted porcine without cell therapy (n = 8); infarcted porcine receiving iPS-CM sheets (n = 7); infarcted porcine receiving SM sheets (n = 7); infarcted porcine receiving MSC sheets (n = 7)). A, Left ventricle ejection fraction (LVEF) post infarction; there were no differences in the baseline value among the groups after 1 month. NS, no significant difference. All cell therapy groups showed a similar increase in LVEF 2 months post cell therapy ($^{\#}P < 0.05$). The LVEF was higher in the hearts with cell therapy when compared with those without cell therapy after 2 months ($^*P < 0.05$). B, LV end diastolic volume was increased in each group relative to the baseline value after 2 months ($^{\#}P < 0.05$). C, LV end systolic volume in the hearts receiving iPS-CM was lower than that in other cell types at 2 months ($^{\#}P < 0.05$); however, it was increased in the hearts of control animals ($^{\#}P < 0.05$). D, The iPS-CM therapy alleviated global wall stress when compared with that in the animals transplanted with other cell types and the control group ($^*P < 0.05$).

SDC, <http://links.lww.com/TP/B613>) 1 month after MI and 2 months after cell transplantation. The LVEF varied across groups; the value increased after cell therapy; however, it decreased in the control group for 2 months after the sham operation (Figure 2A). The increase in LVEF was greater in the iPS-CM group than that in the other cell treatment groups ($P = 0.08$ vs SM group; $P = 0.07$ vs MSC group), although the difference was not statistically significant. All the groups showed a progressive dilation in the LV end diastolic volume (LVEDV) (Figure 2B). However, there was a trend toward attenuation of smaller dilation in the LV end systolic volume (LVESV) in the hearts treated with the iPS-CM when compared with that of other cell types (Figure 2C). Moreover, the iPS-CM reduced systolic myocardial wall stress to a greater degree than the other cell types (Figure 2D).

Regional Cardiac Function

The effects of iPS-CM therapy were most apparent in the cardiac MRI analysis of regional cardiac function (Figure 3 and Figure S5, SDC, <http://links.lww.com/TP/B613>). The LV wall thickening in the IZ of cell-engrafted hearts increased in the iPS-CM group but not in the SM or MSC group (Figure 3A). Although the myocardial wall stress in the noninfarcted region (RZ) was comparable among groups (Figure S5A, SDC, <http://links.lww.com/TP/B613>), the hearts that received the iPS-CM showed significant decline in the BZ and IZ (Figure 3B and Figure S5B, SDC, <http://links.lww.com/TP/B613>).

Two-dimensional speckle-tracking echocardiography was performed to quantify the regional systolic function (Figure 3 and Figure S6, SDC, <http://links.lww.com/TP/B613>). The

radial, longitudinal, and transverse strains were used to assess the cardiac wall motion. Two stable and well-defined consecutive cardiac cycles were acquired. The mid-anteroseptal area imaged in the long-axis view was considered as the IZ. The inferior midsegment imaged in the same view was considered as the noninfarcted region (RZ). The peak strain was defined as the highest strain value obtained throughout the cardiac cycle, and it represented the regional systolic function in each segment. The systolic function at the IZ of hearts transplanted with the iPS-CMs improved 1 and 2 months after cell therapy (Figure 3C and Figure S6A, B, SDC, <http://links.lww.com/TP/B613>). Myocardial infarction led to a delay in the systolic strain in the injured myocardium, resulting in dyssynchronization between the infarcted and noninfarcted areas. The time to peak radial strain in each of these areas was calculated. The dyssynchrony was evaluated according to time discrepancies between the 2 segments. The dyssynchrony index gradually improved in animals treated with the iPS-CMs but not in the other groups (Figure 3D). Thus, the iPS-CM therapy blocks the progression of heart failure, as evidenced by reduced LVESV, improved global LV function (LVEF and global wall stress), increased regional wall motion (peak strain in the IZ), and reduced regional wall stress when compared with those of the treatment with other cell types.

iPS-CM Therapy Improves Myocardial Oxygen Consumption After MI

We investigated whether the functional improvements observed in the iPS-CM group were accompanied by improved oxygen consumption and myocardial bioenergetics. The PET

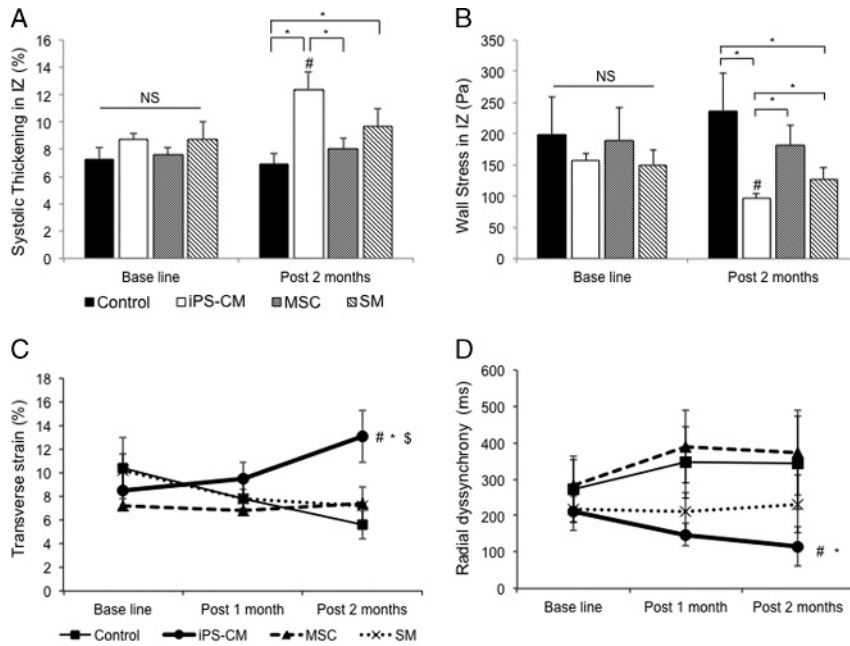


FIGURE 3. Effects of the transplanted induced pluripotent SC-derived cardiomyocytes (iPS-CM), skeletal myoblast (SM), and mesenchymal stem cell sheets on regional cardiac function. A, B, Quantitative assessment of wall thickening and myocardial wall stress in the IZ by cardiac MRI. A, Regional wall thickening in the IZ increased to a greater degree relative to that of the control animals by the iPS-CM therapy when compared with that of the SM and MSC therapies ($^{\#}P < 0.05$). B, Regional myocardial wall stress in the IZ was alleviated by the iPS-CM therapy as compared with that of the other cell therapy groups and controls ($^{\#}P < 0.05$). C, D, Two-dimensional speckle tracking of the transverse strain in the IZ (C) and radial dyssynchrony between the IZ and RZ (D). The transverse strain was improved by the iPS-CM therapy ($n = 7$) but was aggravated in the SM ($n = 7$), MSC ($n = 7$), and control ($n = 8$) groups ($^{\#}P < 0.05$ vs SM group; $^{\#}P < 0.05$ vs MSC group; $^*P < 0.05$ vs control group). Dyssynchrony was defined as a time difference between the anterolateral IZ and posterior RZ segmental peak strain ($^{\#}P < 0.05$ vs MSC group; $^*P < 0.05$ vs control group).

with radiolabeled ^{11}C acetate has been used to measure the rate of oxidative metabolism, which is directly related to myocardial oxygen consumption. Evaluating this and cardiac efficacy in conjunction with ventricular performance can provide insight into the effects of cell therapy on the LV function. The measurements were made under rest conditions and elevated cardiac work state induced by catecholamine. The k_{mono} increased in the iPS-CM group as well as in the other cell therapy groups under high cardiac workload (Figure 4A), although the change was not statistically significant. On the contrary, the CE improved in the pigs treated with the iPS-CM; however, it was unchanged in the other groups (Figure 4B). These data indicate that the iPS-CM therapy improves myocardial bioenergetics.

iPS-CM Therapy Enhances Vasculogenesis in the IZ and BZ

Myocardial infarction caused a significant loss of vascularity, as evidenced by the lack of CD31 positivity in the infarcted hearts of control pigs. To determine whether cell therapy could stimulate angiogenesis and thereby promote tissue repair, we quantified CD31+ vascular structures and arterioles coexpressing CD31 and smooth muscle actin (SMA) 2 months after cell therapy (Figure 5A–D). The vascular density (determined as the number of CD31+ vascular structures/ mm^2) was greater in the cell therapy groups than in the control group in the IZ (Figure 5E) and BZ (Figure S7A, SDC, <http://links.lww.com/TP/B613>). The ratio of arteriolar capillaries within the vascular structures (ie, SMA+/CD31+

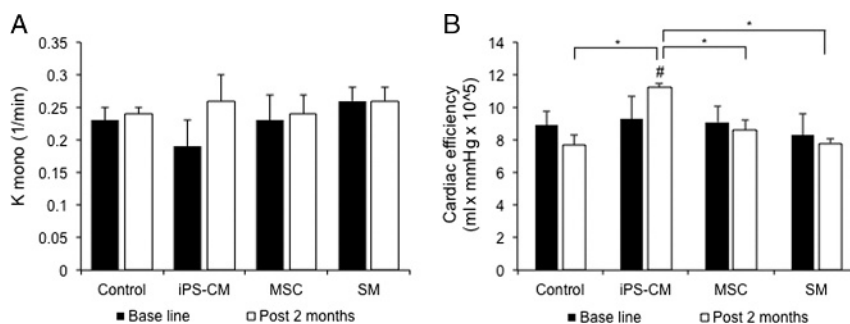


FIGURE 4. Measurement of in vivo myocardial oxidative metabolism based on the C-11 clearance rate under a high cardiac work state induced by catecholamine stimulation ($n = 3$ each for infarcted porcine without cell therapy, infarcted porcine receiving induced pluripotent SC-derived cardiomyocytes (iPS-CM) sheets, infarcted porcine receiving skeletal myoblast (SM) sheets, and infarcted porcine receiving mesenchymal stem cell sheets). A, Acetate clearance rate (k_{mono}) as a measure of global cardiac oxygen consumption. B, CE increased by up to 21% in the hearts transplanted with the iPS-CM sheets ($^{\#}P < 0.05$ vs baseline; $^*P < 0.05$ vs other groups).

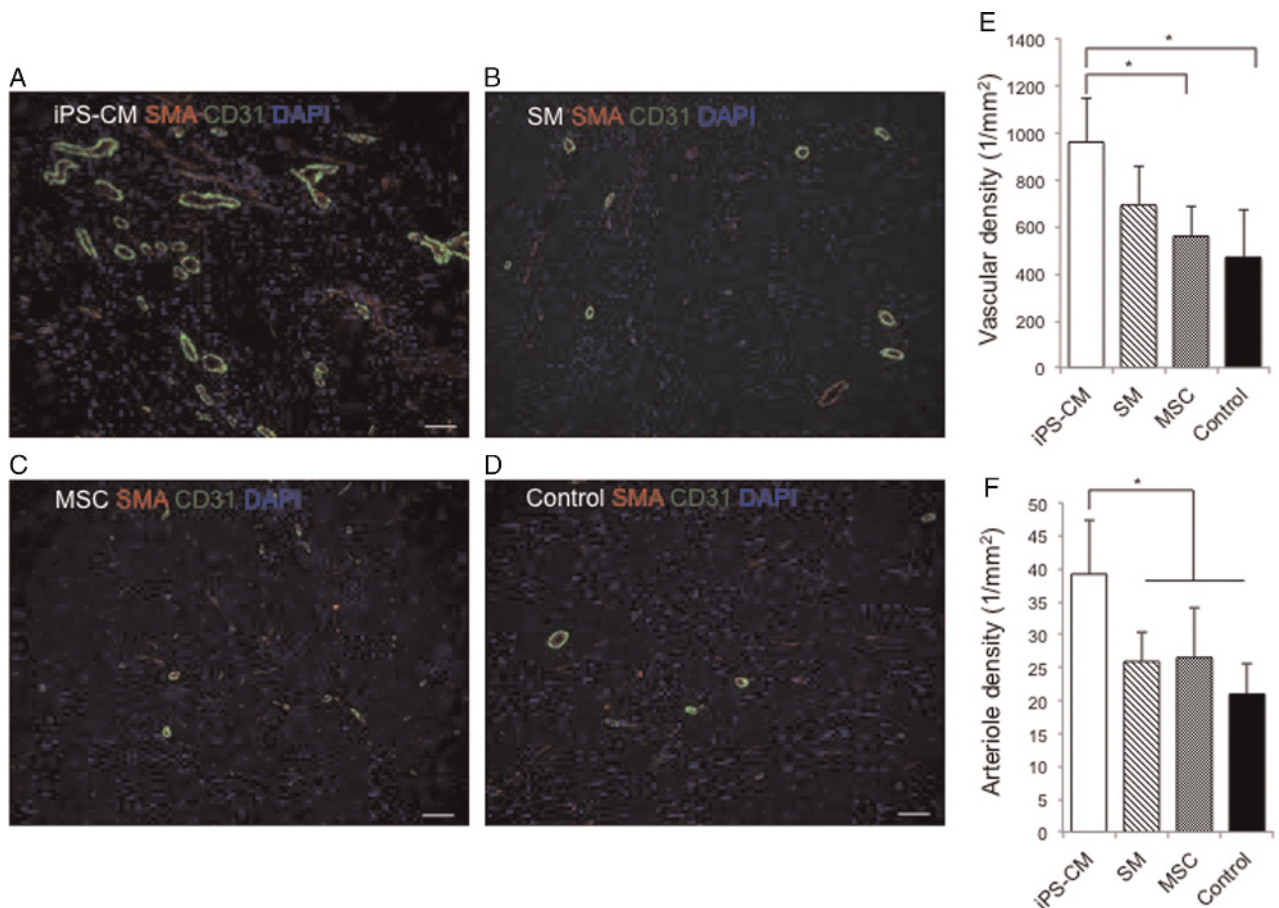


FIGURE 5. Induced pluripotent SC-derived cardiomyocytes (iPS-CM) therapy enhances vasculogenic response. Vascular and arteriole densities were evaluated 2 months after cell therapy in sections from the IZ in the hearts of animals from the (A) induced pluripotent SC-derived cardiomyocytes (iPS-CM), (B) skeletal myoblast (SM), (C) mesenchymal stem cell, and (D) control groups by immunofluorescence labeling of SMA (red) and CD31 (green). E, Vascular density was determined by counting the CD31+ vascular structures. F, Arteriole density was determined by counting the vascular structures expressing both CD31 and SMA (* $P < 0.05$). Scale bar, 50 μm .

vascular structures) was higher in the iPS-CM group than in the control group in the IZ (Figure 5F) and BZ (Figure S7B, SDC, <http://links.lww.com/TP/B613>). These data suggest that the iPS-CM therapy promotes neovascularization and arteriolar capillary formation.

iPS-CM Therapy Reduces CM Apoptosis

We investigated whether cell transplantation has a cytoprotective effect against tissue injury caused by MI. To assess this possibility, tissue sections from the IZ were immunolabeled for cTnT to identify CMs and were analyzed for the presence of single-strand (ss)DNA, a marker of apoptosis (Figure 6A–D). The proportion of cells positive for both ssDNA and cTnT was the highest in the hearts of control animals. Furthermore, the ratio of ssDNA+ to cTnT+ cells was lower in the hearts from the iPS-CM group than that in the hearts from the other groups (Figure 6E). Thus, the iPS-CM therapy exerts cytoprotective effects by suppressing CM apoptosis in the infarcted area, which may be accompanied by a reduced wall stress and improved systolic function.

DISCUSSION

This study presents several important findings. First, we demonstrated, in an immunosuppressed large animal model of MI, that xenogeneic epicardial transplantation of iPS-CMs, SMs, and MSCs improved cardiac function, which

was the most apparent with iPS-CM transplantation. Second, although the increase in angiogenesis in the ischemic region was comparable across treatments, the transplantation of iPS-CMs caused a more significant increase in capillary density in these regions than that of the other cell types. This along with the observation that the number of nuclei per CM was unchanged suggests that CM apoptosis was inhibited to a greater degree by the iPS-CMs. Finally, the epicardial iPS-CM transplantation with bioengineered cell sheets reduced wall stress in both the whole heart and the ischemic region; this was associated with the preservation of cardiac energy, as determined by cardiac oxygen consumption.

During MI, structural and functional abnormalities occur in the BZ and IZ. The surviving BZ myocytes then spread to the surrounding regions of healthy myocardium until the entire LV is impaired,¹³ with a resultant increase in wall stress. The iPS-CM transplantation reduced global and regional LV wall stress in control animals. There was also a trend toward lower LVESV in the iPS-CM group although the values were similar across the groups. In the present study, with the iPS-CMs therapy, the regional functional recovery and dyssynchrony recovery in the infarcted area were better than those with the SM and MSC therapies. The physiology underlying the improvement in systolic function was not clear in the present study because we did not find histological evidence of cell-cell contacts between the

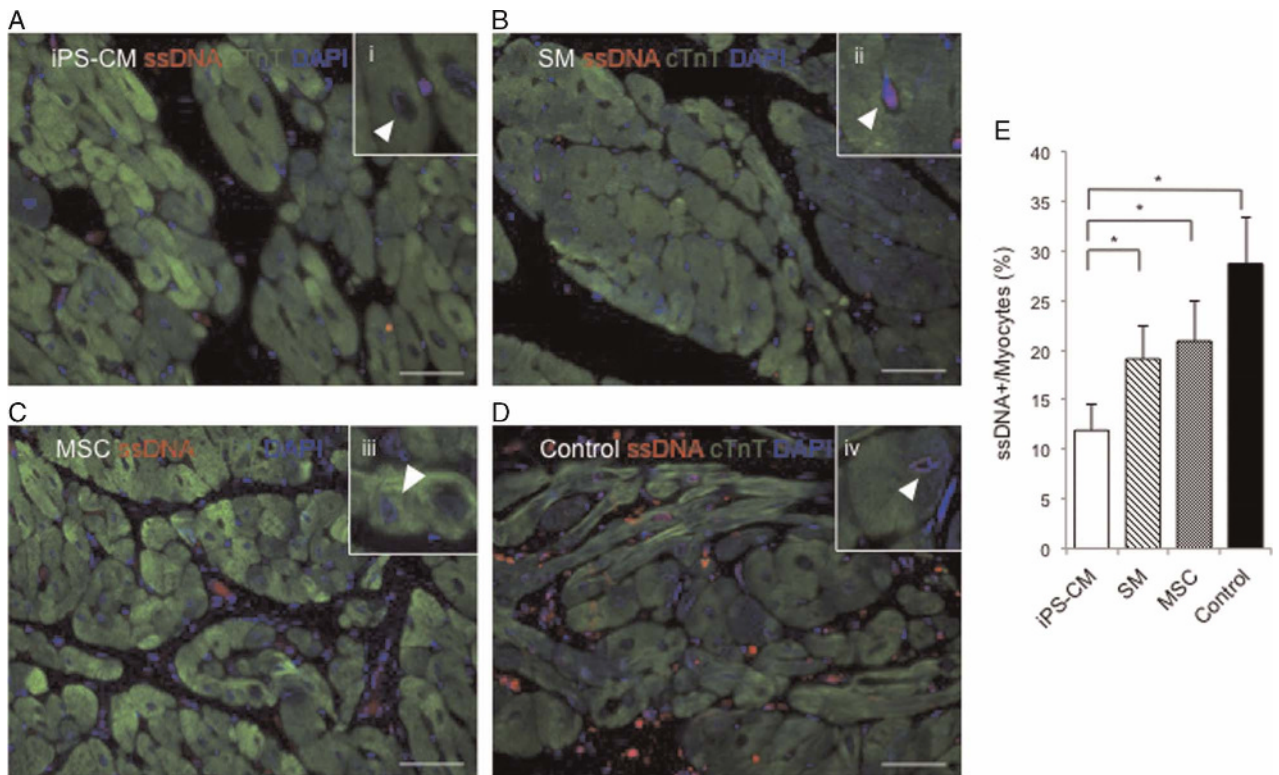


FIGURE 6. Induced pluripotent SC-derived cardiomyocytes (iPS-CM) therapy reduces CM apoptosis. Apoptotic CMs were identified in sections from the IZ in the hearts from animals in the (A) induced pluripotent SC-derived cardiomyocytes (iPS-CM), (B) skeletal myoblast (SM), (C) mesenchymal stem cell, and (D) control groups by fluorescence immunolabeling of ssDNA (red). CMs were visualized by fluorescence immunolabeling cardiac troponin T (cTnT) (green); nuclei were counterstained with 4',6-diamidino-2-phenylindole (DAPI) (blue). (i-iv) Representative ssDNA+ myocytes under high magnification in figure insets; denoted by arrowheads. E, CM apoptosis was quantified as the percent of cardiac troponin T (cTnT)-positive cells that were also positive for ssDNA ($*P < 0.05$). Scale bar, 50 μ m.

graft and host myocytes. One reason why the transplanted CMs were not detected in this study is the poor survival rate of transplanted cells. It has been previously reported that the transplanted CMs have a survival rate of ~15%.¹⁴ Cell loss may result from physical strain after transplantation, hypoxia, or cell washout through the vascular or lymphatic system. Recent studies have shown promising approaches to improve the survival of cells transplanted into damaged hearts. For instance, to prevent starvation due to hypoxia and nutrient deficiency, cells have been transplanted along with the omentum flap.¹⁵ The iPS-CMs have also been cotransplanted with the iPS-derived vascular cells, which form new capillaries between the grafts and host myocardium.¹⁶ Additionally, the major histocompatibility complex-matched iPS cells do not elicit a host immune response.¹⁷

Although we did not observe robust retention of transplanted cells in this study, the iPS-CMs as well as SMs and MSCs improved systolic function. The beneficial effects of cell transplantation on cardiac function have been attributed to paracrine signaling mechanisms that inhibit CM apoptosis,¹⁸ modulate inflammation,¹⁹ and promote angiogenesis.²⁰ In the present study, the capacity of iPS-CMs, SMs, and MSC to release cardiac protective factors, such as vascular endothelial growth factor (VEGF), stromal derived factor-1 (SDF-1), and insulin-like growth factor-1 (IGF-1) was investigated in vitro. The analysis of conditioned medium of iPS-CMs, SMs, and MSC cultures by the enzyme-linked immunosorbent assay revealed that the concentration of SDF-1, VEGF, and IGF-1 was not significantly different among the

cell types (Figure S8, SDC, <http://links.lww.com/TP/B613>). This indicates the paracrine effect of the iPS-CMs and other somatic cell therapies. The results of histological analyses revealed that the hearts transplanted with the iPS-CMs showed increased vasculogenesis and decreased apoptosis when compared with the other cell types. The reason for this disparity is not clear. However, it may be related to VEGF and insulin-like growth factor-1 secretion, which was stimulated by the iPS-CMs, but not by other cell types, when the cells were cultured under hypoxic conditions and subjected to cyclic mechanical stretch, as previously reported.²¹

It is not known how the impairment in cardiac bioenergetics contributes to cardiac dysfunction. Using radiolabeled C-11 acetate to noninvasively monitor myocardial kinetics by PET,^{22,23} we observed a reduction in myocardial oxygen consumption in control hearts that was reversed by the treatment with iPS-CMs, and was accompanied by an improvement in contractile function. This increase in cardiac bioenergetic efficacy is in agreement with the findings of earlier studies, which reported that the factors responsible for myocyte overstretch and increased wall stress also caused a decline in contractile function²⁴ and that targeting these factors improves myocardial ATP hydrolysis/synthesis in the infarcted area.¹⁶ The in vivo mechanisms may involve multiple signaling pathways that interact to modulate the balance between energy demand and supply in order to maintain contractility.²⁵ Such mechanisms may increase the capillary density along with myocyte nuclear density, which could maintain the capillary-to-myocyte ratio in the hearts treated

with the iPSC-CMs, but not in those treated with the SMs and MSCs, thereby providing oxygen to the damaged tissue. Further studies are needed to identify the molecular pathways involved in the beneficial effects of iPSC-CM cell transplantation on cardiac bioenergetics.

The present study and the findings of previous studies demonstrate that the CMs are a suitable for cell-based therapy. The iPSC can be induced to differentiate into CMs *in vitro*; however, purifying the latter from a heterogeneous cell population remains a challenge.²⁶ The rate of CM differentiation was about 65% with our protocol. In a mixed cell population, CM survival can be promoted and the quality of CM bioproducts enhanced by noncardiac cells (eg, fibroblasts).^{27,28} There are always safety concerns, especially regarding the potential tumorigenicity of SC transplantation. To evaluate its capacity to divide in the cell sheet, we investigated Ki-67 expression that is correlated with cell proliferation and is a prognostic marker of various cancers. A few cells were expressed in the iPSC-CM sheet as well as in the SM and MSC sheets (data not shown). These results are consistent with the findings of a previous study, which reported that the cell-cell contacts inhibit the proliferation of cultured cells.²⁹ The relationship between the iPSC-CM differentiation level and the engraftment after cell transplantation was investigated using immunodeficient mice.³⁰ This study reported that iPSC-CMs purified on day 20 from the initiation of differentiation had a high engraftment rate than those purified on day 8 of day 30. These results suggest that further investigations are warranted to explore the optimal differentiation stage (neither too immature nor too close to mature) to enhance engraftment rate and maximize the therapeutic efficacy. A limitation of the present study is that we used different species for the transplanted human cells and the recipient animals. Interspecies differences may influence the survival rate of transplanted human iPSC-CMs, SMs, and MSCs, although we used a combination of 3 immunosuppressive agents after cell transplantation.

In this study, the transplantation of iPSC-CMs, SMs, and MSCs improved global contractility. However, the regional functioning was improved to a greater extent by the treatment with iPSC-CMs when compared with that of the treatment with SMs and MSCs, even with limited cell engraftment 2 months after treatment, suggesting that the iPSC-CMs stimulated neovasculogenesis, and exhibited cytoprotective effects. Our findings indicate that the iPSC-CM transplantation is an effective therapeutic approach for repairing severely damaged myocardium.

REFERENCES

- Porrello ER, Mahmoud AI, Simpson E, et al. Transient regenerative potential of the neonatal mouse heart. *Science*. 2011;331:1078–1080.
- Pasumarthi KB, Field LJ. Cardiomyocyte cell cycle regulation. *Circ Res*. 2002;90:1044–1054.
- Hamshere S, Choudhury T, Jones DA, et al. A randomised double-blind control study of early intracoronary autologous bone marrow cell infusion in acute myocardial infarction (REGENERATE-AMI). *BMJ Open*. 2014;4:e004258.
- Bolli R, Chugh AR, D'Amario D, et al. Cardiac stem cell in patients with ischemic cardiomyopathy (SCIPIO): initial results of a randomized phase 1 trial. *Lancet*. 2011;378:1847–1857.
- Dib N, Dinsmore J, Lababidi Z, et al. One-year follow-up feasibility and safety of the first U.S., randomized, controlled study using 3-dimensional guided catheter-based delivery of autologous skeletal myoblasts for ischemic cardiomyopathy (CAuSMIC study). *JACC Cardiovasc Interv*. 2009;2:9–16.
- Kehat I, Khimovich L, Caspi O, et al. Electromechanical integration of cardiomyocytes derived from human embryonic stem cells. *Nat Biotechnol*. 2004;22:1282–1289.
- Higuchi T, Miyagawa S, Pearson JT, et al. Functional and electrical integration of induced pluripotent stem cell-derived cardiomyocytes in a myocardial infarction rat heart. *Cell Transplant*. 2015;24:2479–2489.
- Okita K, Ichisaka T, Yamanaka S. Generation of germline-competent induced pluripotent stem cells. *Nature*. 2007;715:313–317.
- Takahashi K, Tanabe K, Ohnuki M, et al. Induction of pluripotent stem cells from adult human fibroblasts by defined factors. *Cell*. 2007;131:861–872.
- Narazaki G, Uosaki H, Teranishi M, et al. Directed and systematic differentiation of cardiovascular cells from mouse induced pluripotent stem cells. *Circulation*. 2008;118:498–506.
- Minami I, Yamada K, Otsuji TG, et al. A small molecule that promotes cardiac differentiation of human pluripotent stem cells under defined, cytokine- and xeno-free conditions. *Cell Rep*. 2012;2:1448–1460.
- Matsuura K, Wada M, Shimizu T, et al. Creation of human cardiac cell sheets using pluripotent stem cells. *Biochem Biophys Res Commun*. 2012;425:321–327.
- Hu Q, Wang X, Lee J, et al. Profound bioenergetic abnormalities in peri-infarct myocardial regions. *Am J Physiol Heart Circ Physiol*. 2006;291:H648–H657.
- Müller-Ehmsen J, Whittaker P, Kloner RA, et al. Survival and development of neonatal rat cardiomyocytes transplanted into adult myocardium. *J Mol Cell Cardiol*. 2002;34:107–116.
- Shudo Y, Miyagawa S, Fukushima S, et al. Novel regenerative therapy using cell-sheet covered with omentum flap delivers a huge number of cells in a porcine myocardial infarction model. *J Thorac Cardiovasc Surg*. 2011;142:1188–1196.
- Xiong Q, Ye L, Zhang P, et al. Functional consequences of human induced pluripotent stem cell therapy: myocardial ATP turnover rate in the *in vivo* swine heart with postinfarction remodeling. *Circulation*. 2013;127:997–1008.
- Mizukami Y, Abe T, Makimura Y, et al. MHC-matched induced pluripotent stem cells can attenuate cellular and humoral immune response but are still susceptible to innate immunity in pigs. *PLoS One*. 2014;9:e98319.
- Ye L, Chang YH, Xiong Q, et al. Cardiac repair in a porcine model of acute myocardial infarction with human induced pluripotent stem cell-derived cardiovascular cells. *Cell Stem Cell*. 2014;15:750–761.
- Kim SV, Houge M, Brown M, et al. Cultured human bone marrow-derived CD31(+) cells are effective for cardiac and vascular repair through enhanced angiogenic, adhesion, and anti-inflammatory effects. *J Am Coll Cardiol*. 2014;64:1681–1694.
- Kinnaird T, Stabile E, Burnett MS, et al. Marrow-derived stromal cells express genes encoding a broad spectrum of arteriogenic cytokines and promote *in vitro* and *in vivo* arteriogenesis through paracrine mechanisms. *Circ Res*. 2004;94:678–685.
- Yu T, Miyagawa S, Miki K, et al. *In vivo* differentiation of induced pluripotent stem cell-derived cardiomyocytes. *Circ J*. 2013;77:1297–1306.
- Beanlands RS, Bach DS, Raylman R, et al. Acute effect of dobutamine on myocardial oxygen consumption and cardiac efficiency measured using carbon-11 acetate kinetics in patients with dilated cardiomyopathy. *J Am Coll Cardiol*. 1993;22:13989–13998.
- Beanlands RS, Nahmias C, Gordon E, et al. The effects of beta(1)-blockade on oxidative metabolism and the metabolic cost of ventricular work in patients with left ventricular dysfunction: a double-blind, placebo-controlled, positron-emission tomography study. *Circulation*. 2000;102:2070–2075.
- Xiong Q, Ye L, Zhang P, et al. Bioenergetic and functional consequences of cellular therapy: activation of endogenous cardiovascular progenitor cells. *Circ Res*. 2012;111:455–468.
- Pound KM, Sorokina K, Ballal K, et al. Substrate-enzyme competition attenuates upregulated anaplerotic flux through malic enzyme in hypertrophied rat heart and restores tricylglyceride content: attenuating upregulated anaplerosis in hypertrophy. *Circ Res*. 2009;104:805–812.
- Cao N, Liu Z, Chen Z, et al. Ascorbic acid enhances the cardiac differentiation of induced stem cells through promoting the proliferation of cardiac progenitor cells. *Cell Res*. 2012;22:219–236.
- Kolossov E, Bostani T, Roell W, et al. Engraftment of engineered ES cell-derived cardiomyocytes but not BM cells restores contractile function to the infarcted myocardium. *J Exp Med*. 2006;203:2315–2327.
- Iseoka H, Miyagawa S, Fukushima S, et al. Pivotal role of noncardiomyocytes in electromechanical and therapeutic potential of induced pluripotent stem cell-derived engineered cardiac tissue. *Tissue Eng Part A*. 2018;24:287–300.
- Wieser RJ, Oesch F. Contact inhibition of growth of human diploid fibroblasts by immobilized plasma membrane glycoproteins. *J Cell Biol*. 1986;103:361–367.
- Funakoshi S, Miki K, Takaki T, et al. Enhanced engraftment, proliferation, and therapeutic potential in heart using optimized human iPSC-derived cardiomyocytes. *Sci Rep*. 2016;6:19111.